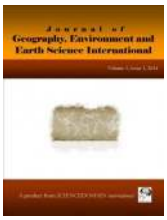

Journal of Geography, Environment and Earth Science International
4(2): 1-17, 2016; Article no.JGEESI.22392
ISSN: 2454-7352

SCIENCEDOMAIN *international*
www.sciencedomain.org

Impact of Refugee Camps on Their Environment A Case Study Using Multi-Temporal SAR Data

Andreas Braun[1*], Stefan Lang[2] and Volker Hochschild[1]

[1]Institute for Geography, University of Tübingen, Rümelinstraße 19-23, 72070 Tübingen, Germany.
[2]Department of Geoinformatics, Z GIS, University of Salzburg, Schillerstraße 30, 5020 Salzburg, Austria.

Authors' contributions

This work was carried out in collaboration between all authors. Author AB processed the data, classified the images, performed the analyses and wrote the draft of the manuscript. Author SL contributed literature research and refined the manuscript. Author VH supervised the study in terms of design, data processing and the performed analyses. All authors read and approved the final manuscript.

Article Information

DOI: 10.9734/JGEESI/2016/22392
Editor(s):
(1) Pere Serra Ruiz, Department of Geography, Universitat Autònoma de Barcelona, Spain.
Reviewers:
(1) Ahmet Sayar, Kocaeli University, Turkey.
(2) Shaikh Md. Babar, D.S.M. College, Parbhani, Maharashtra, India.
Complete Peer review History: http://sciencedomain.org/review-history/12304

Original Research Article

Received 30th September 2015
Accepted 29th October 2015
Published 16th November 2015

ABSTRACT

Monitoring the environment is a key task of remote sensing in particular in areas whose access is difficult or dangerous or where dense cloud cover obscures optical information. This study proposes an assessment of landscape changes related to large refugee camps, where information about environmental conditions is needed by both humanitarian organizations and regional administrations. Our intention is to provide a robust workflow which is applicable for an operational use. The study area is located in Western Kenya hosts a total number of 350.000 people. Images of ERS-2 and Sentinel-1 are used for the assessment of land degradation in a semi-arid savannah between 1997 and 2014.
We expect a relationship between the existence of the refugee camps and the degradation of surrounding landscapes. For this purpose we present an approach which objectively reveals developments in natural resources based on six land-use / land cover classes integrating their relative importance for the ecosystem given by expert-based weights.

**Corresponding author: Email: an.braun@uni-tuebingen.de;*

An index of Natural Resource Depletion (NRD) is calculated using a Random Forest algorithm in order to classify a time series of SAR images and their textures at different spatial scales ($r^2 = 0.71$). Especially large-scale textures turned out to contribute to the classification.
Or results showed a continuous increase of bare soil areas within a radius of five kilometers around the refugee camps and a total decrease of natural resources by 11.8% in the study area. Although the produced NRD maps reveal hot spots of landscape change for selected periods, a clear pattern of land degradation could not be identified and an evident interrelation between the expansion of the camp and the decrease of natural resources has still to be provided.
The proposed approach is applicable to images of other radar sensors as well, such as Sentinel-1 of the European Space Agency which currently collects a multitude of scenes in high spatial resolution. It is therefore suitable for an operational use for the monitoring of land degradation around refugee camps.

Keywords: Remote sensing; refugee camps; land-cover classification; Synthetic Aperture Radar (SAR), land degradation; ERS; Sentinel-1.

1. INTRODUCTION

According to the United Nations High Commissioner for Refugees (UNHCR) the number of people forced to leave their home reached nearly 60 million in the second half of 2015 [1]. The reasons lie in natural disasters such as droughts, floods and land degradations caused by climatic changes as well as in social factors such as poverty, prosecution and armed conflicts [2]. One of the main phenomena challenging the regions affected by immigration are refugee or internally displaced people (IDP) camps where large numbers of displaced people settle down, often close to border at random sites which were not prepared for such enormous influx [3]. Especially in African and the Middle-East camps and temporary settlements are a widespread phenomenon since in the last century [4]. Due to the spontaneous nature of migration host countries often lack the means to plan effective camp structures, while otherwise both refugees and the host population would benefit from a strategic design of infrastructure and social facilities by non-governmental organizations or the UNHCR [5]. In addition, the exact numbers of dwellings and people, the size of the camp and the conditions of the surroundings are not documented throughout and need to be estimated. But the integrity of the environment plays a crucial role for sustaining life in the camp: Not only do the immediate surroundings provide essential resources such as drinking water, firewood, and soils for agricultural use, but also has the refugees' wellbeing and health been found to be dependent from the proximate natural conditions they perceive and are exposed to [6,7]. Further looking, information about the development of both the camp and the environment may better assist the planning process of decision-makers when it comes to land-use and the carrying capacity and vulnerability of ecosystems in the affected regions [8].

While the interdependencies of refugee camps and their social and political environments are already investigated well [9-13], their impacts on the natural surroundings are quite unexplored yet. Although it seems obvious that large camps accelerate land degradation, a clear evidence of their potential adverse effects is currently being discussed [14,15]. This is due to the lack of clear evidence on a relationship between the assumed impact of a camp and other influences on the natural surroundings like climatic or seasonal variations [16].

Remote sensing can provide valuable information about the condition of the earth's surface in general and on the raise and influence of ephemeral settlements such as refugee camps in particular [17]. The ability to collect data through different wavelengths emitted, absorbed and backscattered by surface materials helps observe and monitor large area from space within a short time. One of the most continuing sources for land cover information is the Landsat continuity mission [18]. It started in 1972 and almost constantly delivers images from space since then. Their use for the land-use and land cover classification (LULC) has been widely demonstrated in the past decades [19-24]. Especially the analysis of a series of images over a longer period reveals promising results a thorough understanding of the ongoing processes [25,26]. However, especially regions hosting refugee camps such as Eastern and Equatorial Africa or the Middle East are often affected by a high degree of cloud cover [27-29]

(also see section 2.1.1) that prevent effective time series analyses of land cover change [30].

Instead, satellite images acquired by synthetic aperture radar (SAR) are neither affected by cloud cover nor dependent from daylight. With wavelengths considerably longer than those of optical sensors, using SAR data we detect additional properties of the earth's surface [31]. Their operational use since the 1990ies supported the classification and monitoring of land cover information from space by radar technology [22-35].

To complement the weather- and daylight-depending availability of optical data, this study investigates the potential of SAR data in assessing the environmental conditions around a cluster of refugee camps in Kenya. It presents a strategy for multi-temporal land cover classification to quantify and evaluate the influence of refugee camps on their environment. It closes the gap between qualitative, non-spatial approaches [8,16,36-38], impact assessments using optical satellite data [39-41] and studies based on single-date SAR images [42,43]. Furthermore, the proposed method demonstrates how to use multi-temporal C-band SAR data for LULC classification. This is of particular interest when ESA's Sentinel-1 (S1) satellite data started in the middle of 2015 covers time-series of several years.

2. MATERIALS AND METHODS

2.1 Study Area

Dadaab is a settlement in Garissa County, Western Kenya, consisting of five separate refugee camps (see Fig. 1, main map). The first of them were constructed in the early 1990s as a consequence of the civil war in Somalia. They are located approximately 100 kilometers from the Somali border and today host a total population of 350.000 people, which made them the largest refugee camp in the world in 2015 [44] (see Fig. 1, overview map). The climate can be described as hot and arid with constant temperatures above 30 degrees (BWh according to the Köppen-Geiger classification scheme). There are two rainy seasons from March to April and September to January with up to 5 rainy days per month. Due to a total annual rainfall amount of 370 mm most rivers are only seasonal. The terrain is flat and has sandy and nutrient-poor soils [45] mainly covered by deciduous bush land consisting of *Acacia-Commiphora* shrubs and thicket with scattered patches of grassland and seasonally swampy areas [46].

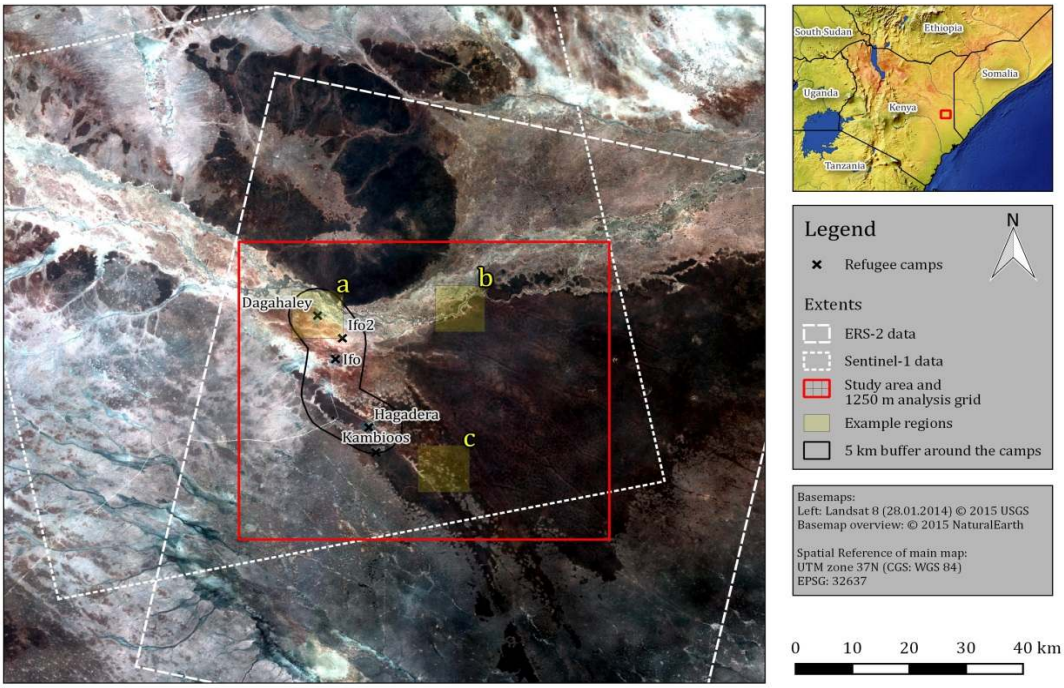

Fig. 1. Study area: Location and extent of datasets

2.2 Data

2.2.1 Satellite imagery

Optical satellite data in this region is often affected by cloud cover. We investigated all available Landsat images of our study area since 1972. A total number of 388 scenes are found in the archive of the US Geological Service (USGS). 373 of them show a cloud cover below 80%, 286 are below 50% and 82 scenes remain with a cloud cover below 5%. While altogether this is still a considerable number (21%), it means that statistically every fifth scene suits well for the envisaged classification purposes. For this reason our study aims to use SAR data alone. We chose the European Remote Sensing Satellites ERS-1 and ERS-2 launched in 1991 and 1995 by the European Space Agency [47]. The mission was officially declared completed in 2011 when ERS-2 ran out of fuel. Covering 20 years of image acquisitions the data archive provides sufficient records to address our research aims. In addition, a Sentinel-1 scene dated 2014 was used due to the fact that the camps in Dadaab region are still in operation. Both Sentinel-1 and ERS are C-band radar sensors operating at a VV polarization and therefore deliver comparable imagery [48].

We tried to ensure that the images of each study area remain comparable in terms of seasonal variation. With SAR backscatter being dependent from soil moisture we selected images acquired during or close to the rainy seasons (see Table 1). Since no data is available before 1997 the setup of the camps since 1991 could not be completely documented. The Sentinel-1 image was acquired in ascending mode while all others were acquired in descending mode. This has an impact when comparing and interpreting results gathered from these data.

2.2.2 Preprocessing

ERS scenes were provided by ESA as Single Look Complex Image products (SLC). The following preprocessing steps were performed: Removal of Antenna Pattern (including removal of replica pulse power and ADC correction) and radiometric terrain flattening (resulting in terrain-flattened Gamma-Naught (γ^0 [49]). This operation minimizes distortions in backscatter intensity caused by the incidence angle on local topography. The scenes were orthorectified by the Range-Doppler algorithm which corrects geometrical distortions caused by the side-looking geometry of the sensor [50]. We did not apply any speckle filtering in order to preserve the original image textures. In classifications based on SAR texture alone accuracies have been reported to drop when speckle removal was employed [51,52]. During the reprojection all scenes were resampled to a common ground resolution of 12.5 meters.

In order to derive additional information layers for classification, we computed image textures based on the Grey-Level Co-Occurrence Matrix (CLCM) [53]. Texture images consist of simple (*Cluster Prominence*, *Cluster Shade*, *Correlation*, *Energy*, *Entropy*, *Haralick Correlation*, *Inertia* and *Inverse Difference Moment*), advanced (Difference Of Entropies, Difference Of Variances, IC1, IC2, Mean, Sum Average, Sum Entropy, Sum Variance and Variance) and higher order (Grey-Level Nonuniformity, High Grey-Level Run Emphasis, Long Run Low Grey-Level Emphasis, Low Grey-Level Run Emphasis, Run Length Nonuniformity, Run Percentage, Short Run High Grey-Level Emphasis and Short Run Low Grey-Level Emphasis). We used kernels of 3, 25 and 69 pixels for the generation of these textures, leading to patterns emerging at different spatial scales. In order to select the most suitable information layers in the subsequent steps, we computed a total of 79 texture images for each of the five data sets for the analysis of the respective time step.

As Table 1 shows, we used two optical scenes from the Landsat mission for training purposes. We chose the year 2000 for Landsat because of the small temporal gap between the scene and the SAR image (5 days) and its comparably low cloud cover (26%). We then manually collected 1500 sample points for six different land-use and land cover classes (see section 2.3). They were evenly distributed over the whole study area and thus representative for the statistical spatial occurrence of each class.

Table 1. Data sets used in this study

Date	Satellite	Remarks
04 Oct1997	ERS-2	descending
18 Sep 2000	Landsat TM	reference for 18 Sep 2000
23 Sep 2000	ERS-2	descending
17 Sep 2005	ERS-2	descending
09 Jan 2010	ERS-2	descending
27 Dec 2014	Sentinel-1	ascending
07 Jan 2015	Landsat OLI/TIRS	reference for 27 Dec 2014

2.3 Image Classification

For the definition of land-use and land cover classes we chose the Land Cover Classification System (LCCS) proposed by the FAO [54]. It is scale-independent, standardized and widely approved for mapping purposes. Table 2 lists the classes used for our study area. As the vegetation in the study area is widely homogenous in the scale of investigation we only discriminated between non-vegetated classes (*built-up areas*, *bare soils* and *intermittent streams*) and natural vegetation cover of different densities: While *floodplain* is restricted to temporarily flooded areas around the stream channel and covered by single short bushes, *shrubland* refers to terrestrial woody vegetation with a coverage below 65% and *thicket* above 65% respectively. Between the bushes patches of grass and mosses can occur loosely. SAR information can cope with ecosystems of this type due to its sensitivity to roughness and wetness of the surfaces as well as to the volume of the objects such as the described bushes [55,56].

The additional texture layers described in section 2.2.2 reveal a variety of surface characteristics and patterns on different spatial scales. The use of various filter sizes enhances structures ranging over a multitude of pixels and therefore creates information inherent in the image which is not visible to the human eye at first sight. Still, as some of the texture measures are based on related geometrical and mathematical principles, the produced layers also bear redundant information. We therefore employed a classification method that fulfills the following criteria: (1) incorporation of raster information of different units and therefore different ranges of values, (2) handling of large numbers of datasets in an efficient and time-saving way, and (3) selecting those parts of probably redundant information which are of best use for the classification.

Machine learning techniques detect patterns within ordinal data (the training data set) for a later classification of untrained data [57]. In order to make best use of the many input rasters we chose the Random Forest (RF) algorithm [58]. Our training data set consists of the 1500 sample points which contain the assigned class as well as the texture images. By creating a large number of different and uncorrelated regression trees [59], the training data is systematically searched for statistical patterns in order to split the input values into separable classes. Outcomes of different regression trees are then ensembled to a final result. We used 50 separate trees for training purposes with each tree composed of 9 randomly selected input layers (as the rounded up square root of the total number of 79 input rasters). Herewith, RF identifies those raster layers that describe the training data best. A model is then created which can be applied to the input texture rasters in order classify each pixel according to its texture statistics.

Our RF model was built with the training samples collected from the optical information of the Landsat TM scene from 18 Sep 2000 with a training accuracy of 65.8%. The latter means that the algorithm can explain the distribution of the training classes by about 66%. This seems comparably low, but it is caused by semantic similarities of the classes containing vegetation, while the critical classes (*camp* vs. *shrubland*) remain distinct.

The created RF model was subsequently applied to the input rasters of the years 1997, 2005 and 2010. The S1 scene had to be trained separately by additional training samples collected from a Landsat scene due to radiometrical discrepancies and the descending track.

Table 2. Land-use and land cover classes

Class name	LCCS Code	Relative importance (see 2.4)
Refugee camp or settlement	5003-13	0,000
Bare rocks or soil	6005-6	0,059
Intermittent streams and channels	8003-1	0,235
Floodplain	40011	0,176
Shrubland	20021	0,235
Thicket	2001	0,294

2.4 Assessing the Environmental Impact

We chose two measures for assessing the environmental impact of the camps. The first one is the change in area covered by bare soil. As observable in the vicinity of the camps this is a first indicator of land degradation around the settlements. We digitized a line around the camps, reaching from Dagahaley in the north over Ifo2 and Ifo along the road to Hagadera in the south. Camp Kambioos was excluded in this

case as it did not exist until 2011. The line was then buffered by a distance of 5000 m to delineate an area under likely direct influence around the refugee camps. Amnesty International reports that refugees cover distances up to 10 kilometers around their camps for the collection of firewood [60,61].

The second indicator is a slightly modified version of the *Weighted Natural Resource Depletion Index* (NRDw index) proposed by Hagenlocher et al. [39]. It aggregates the percentages of land-use classes on a coarser spatial scale and evaluates their temporal change based on weights according to their social and ecological importance. In our case, we focused on the latter, ecological importance, and did not explicitly consider social aspects. The weights given in Table 1 were assessed by two regional experts with ecological and humanitarian background as follows: Each of the five land-use / land cover classes was assigned a value from 0 to 5 according its relative ecologic importance in the study area, while zero means no particular ecological relevance and 5 reflects a very high relevance: Refugee camp or settlement (0), bare rocks or soil (1), intermittent streams and channels (4), floodplain (3), shrubland (4) and thicket (5). Each weight was then divided by the sum of all weights in order to get each the relative importance (RI) of each class.

We used an analysis grid with a spacing of 1250 meters (one hundred times the spatial resolution of the input SAR textures) and assessed the relative area of each land-use and land cover class per grid cell. Areas and RIs of each class occurring in a grid cell were then multiplied and aggregated to a single index value of natural resources (NR) per grid cell. Accordingly, the development of land-use and land cover is no longer analyzed at the pixel level but at an aggregated spatial index of 1250 meters representing the relative presence of inherent classes. Changes in the ecological value of a grid cell can then be described by an increase or decrease of the NR (natural resource depletion, NRD). An example of this calculation is given in Fig. 2. Negative NRD values indicate loss of resources while positive values represent gain within the corresponding grid cell.

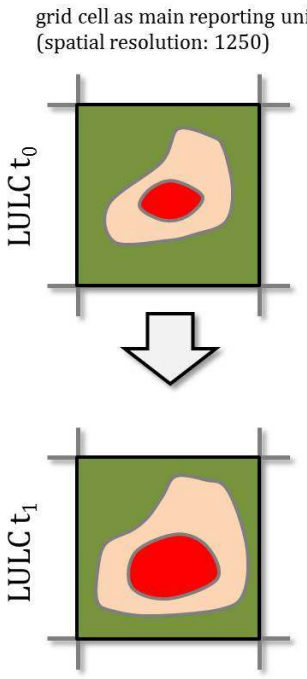

Class	Area	Relative Importance (RI)	Natural Resources (NR)
Refugee camp or settlement	10 %	0,000	0,1 * 0,000 = **0,000**
Bare rocks or soil	20 %	0,059	0,2 * 0,059 = **0,012**
Shrubland	70 %	0,235	0,7 * 0,235 = 0,165
			∑ 0.177

Class	Area	Relative Importance (RI)	Natural Resources (NR)
Refugee camp or settlement	20 %	0,000	0,2 * 0,000 = **0,000**
Bare rocks or soil	30 %	0,059	0,3 * 0,059 = **0,018**
Shrubland	50 %	0,235	0,5 * 0,235 = 0,118
			∑ 0.136

NRD = $t_1 - t_0 = 0,136 - 0,177 = -0,041 =$ **-4,1%**

Fig. 2. Calculation of the weighted Natural Resource Depletion (NRD) index

This approach has several advantages: (1) output maps can be interpreted quick and easily while detailed knowledge about the initial land-use classes is no longer required, (2) single misclassified pixels as often shown by SAR images due to speckle have little to zero effect on the NR of a cell, and (3) expert-based weights (RIs) are integrated and adjustable according to the research questions (environmental vs. social impact). Additionally, as all RIs shown in Table 1 sum up to 1, NR values can be directly interpreted as percentages of positive or negative ecological development. In our case, a decrease by 100 % would indicate a cell formerly covered by thicket alone (most valuable class) which was completely substituted by a refugee camp (least valuable class) within one time step.

3. RESULTS AND DISCUSSION

3.1 Image Classification

The r^2 of the trained RF model is 0.65 and gives a fist estimate of the reliability of the algorithm. As already discussed in section 2.4 coarse misclassifications cannot be expected. Fig. 3 gives three visual examples of the classification at selected places. Their locations within the study area are indicated as yellow squares in Fig. 1. The RF model based on SAR textures was able to clearly discriminate camp areas from their local environment which is bare soil in most cases. It furthermore accomplished to detect shrubland of different densities and soil conditions. It can also be observed that the SAR based results still contain some pixelated areas, which can be explained by the use of textures of different sizes. These mostly occur at transitions between two similar classes such as 'stream channels' and 'floodplains' or shrubland and thicket. As these transitions are also a continuum in nature, sharp borders would not be desirable in any case.

In order to further proof the accuracy of our approach we manually digitized 600 further validation points based on the Landsat scene from the year 2000. This was undertaken by a different person from the one who collected the training samples as described in section 2.2.2 in order to grant for an unbiased and objective interpretation. Table 3 shows the confusion matrix based on validation samples and the classified map for the year 2000. It reveals an overall accuracy of 71 % which is acceptable for a classification based on SAR data alone [62]. It furthermore shows high user's accuracies (also interpreted as reliability of the map) for the two classes *camp* and *bare rocks or soil*. Most of the misclassified samples result from the similarity of *shrubland*' and *thicket* or *stream channels* and *floodplain*. As already mentioned, these errors however only play a minor role for the later calculation of the natural resources (NR).

3.2 Area Affected by the Refugee Camps

Fig. 4 shows the temporal development of land-use and land cover classes within the direct vicinity of the camps. It considers all areas within a distance of 5000 meters from the demarcation line as described in section 2.4 and includes an area of 360 km² (see Fig. 1). As one main indicator for land degradation a continuous increase of *bare rocks or soil* can be attested. It rises from nearly 60 km² in 1997 to 83 km² in 2014. This can be explained due to progressive soil degradation directly around the camps (see Fig. 3a). A similar but less pronounced development can be observed for the camps themselves which increase from 15 km² to 21 km². The outlier in 2000 can be explained by an overestimation of camp areas due to slightly different moisture conditions which strongly affect

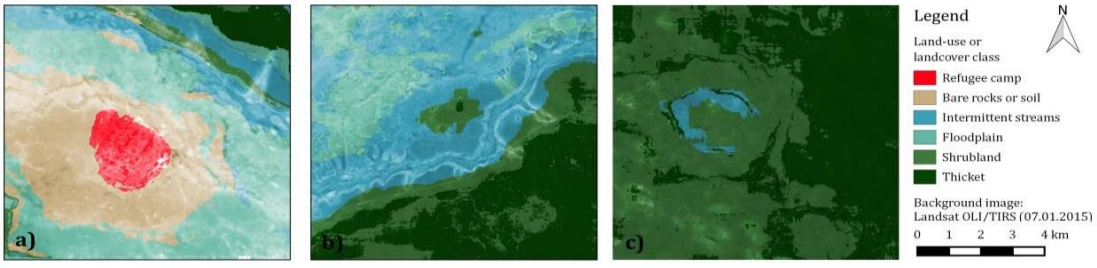

Fig. 3. Selected examples of the land-use / land cover classification. a) Camp Dagahaley (2010), b) Floodplain and temporary streams (1997) and c) Transition from dense to open shrubland and temporarily moist areas

the contrast between the signature of the camp and its surrounding bare soils. Additionally, a nearly steady increase of *shrubland* can be observed.

Indifferent temporal behavior is shown by the two classes related to hydrology. As already shown in Table 3, these classes can change during the year according to rainfall and water discharge. Accordingly, no clear trend can be attested.

Regarding *thicket* a significant decrease is observable from 2010 to 2014. This may be accredited to the different sensor (S1 instead of ERS) and the ascending pass which generally underestimated closed shrubs in the whole image. Consequently, the share of all other classes in 2014 could in fact be slightly smaller.

3.3 Environmental Impact

Fig. 5 shows the calculated NRD values between each of the investigated image pairs. Contrary to our expectations, there is no clear trend visible at first sight. Still, due to the imbalanced spatial distribution of classes in our study area certain areas reveal larger changes than others. At first, land degradation is expressed in the regions around the camps, especially Ifo2 and Hagadera. These negative values are mostly expressed by the extension of *bare soil* areas account of *floodplains* and *shrubland*. Further dynamics can be observed at the edges of the braided river system. Changes in the hydrological system lead to decreasing and increasing of the floodplain as well as to variations of the stream course. Positive development seem widely restricted to the shrubland areas in the eastern part of the study area where open shrubs grow into more dense ones and vice versa.

An overall decrease of natural resources by 11.8% could be detected in the study area between 1997 and 2014. The largest depletion of resources between two observations can be observed within the first period with a NRD sum of -8.17. It is followed by -7.96 for the period between 2010 and 2014 and a clearly lower value of -3.29 for 2000-2005. From 2005-2010 the sum of all NRD values is even positive with 8.13. According to these numbers, the strongest loss of natural resources should have happened during the first 10 years since the opening of the camps which seems plausible. The positive value from 2005-2010 indicates that some parts of the environment were able to recover. According to Fig. 5 these were mainly within the shrubland areas where the vegetation cover became denser again. Since extreme NRD values could also result from rough misclassifications, they strongly influence these sums which therefore should be interpreted with respective caution.

Fig. 6 shows the sum of NRD values for all time increments taken together. It no longer considers temporal evolution in steps but summarizes the whole investigated period. It supports the indications that the largest loss of natural resources was restricted to the areas directly around the mines. Based on the analysis grid an 'impact radius' of two to four cells around each camp can be estimated which corresponds to 2.5 to 5 kilometers. Further strongly affected areas (more than 10% loss) are restricted to the floodplain in the north.

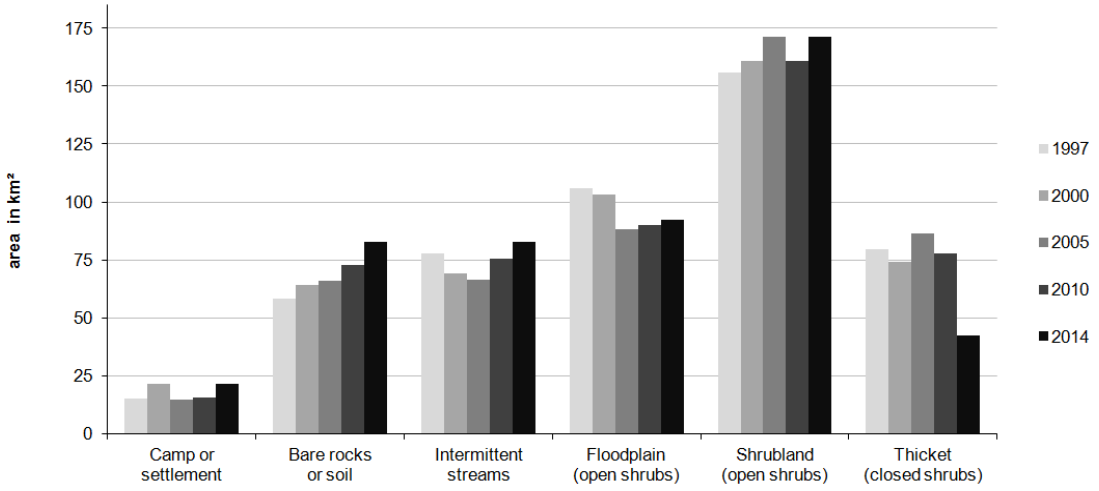

Fig. 4. Change of class areas around the refugee camps from 1994 to 2014

The figure additionally shows that most of the shrubland areas suffered from a slight decrease (light green) and only gained ecological value within the thicket in the eastern part (dark green and blue). The recovery between the camps Ifo2 and Hagadera indicates dismantling of built-up objects along the road connecting these sites but it does not seem to correspond to a specific date when compared to the maps of Fig. 5.

3.4 Validation

The presented results are dependent on several circumstances. With respect to the input data, most reliable results can be achieved when the images are acquired by the same sensor in the same mode during the same time of the year. Due to the fact that SAR sensors area especially sensitive to soil moisture, the role of the seasonal period or even date is essential for image acquisition. Not only do landscapes change within one hydrological year but also can small rainfall events strongly influence the backscattered signal and therefore the derived textures. In our case we had to rely on available scenes from the ERS archive and tried to minimize the 'seasonal window' in which the images were taken. Additionally,

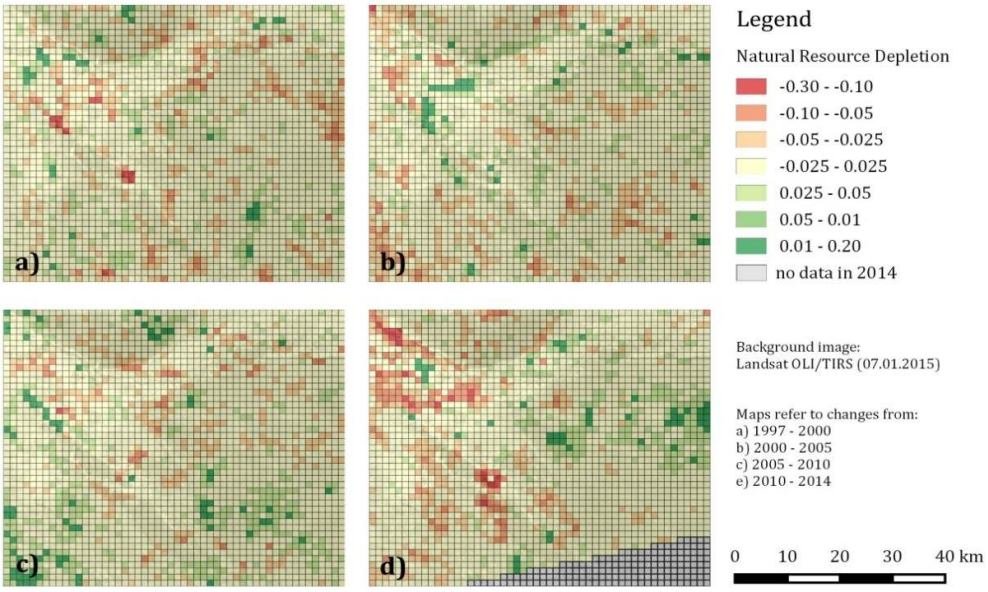

Fig. 5. Environmental developments expressed by the Natural Resource Depletion (NRD) index

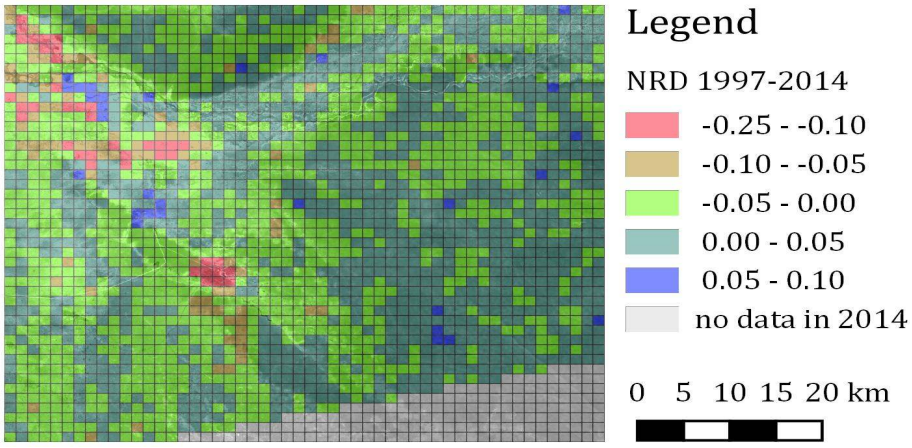

Fig. 6. Severity of Natural Resource Depletion (NRD) per grid cell for the period between 1997 and 2014

Table 3. Accuracy assessment for the map of 2000 validation data

		Camp	Bare soil	Stream	Floodplain	Shrubland	Thicket	UA
map prediction	camp	70	7	1	2	0	0	87,5%
	bare soil	5	80	1	1	0	0	92,0%
	stream	1	0	69	27	7	0	66,3%
	floodplain	0	3	16	53	13	1	61,6%
	shrubland	11	0	3	6	67	32	56,3%
	thicket	3	0	0	1	33	87	70,2%
	PA	77,8%	88,9%	76,7%	58,9%	55,8%	72,5%	71,0%

** PA: Producer's accuracy; UA: User's accuracy*

constant time intervals are advisable. Unfortunately, no images were acquired before and during the arising of the camps in the region beginning in 1991. These would have been supportive in characterizing the undisturbed state of the environment before the human impact. Despite these inconsistencies at the input data level our results are satisfactory. The currently growing archive of SAR data collected Sentinel-1 will serve as an extremely valuable source of information in the future.

Table 4 shows the 15 most important input layers for the generation of the RF model. Their *feature importance* is expressed as the relative rank of an information layer used as a decision node in a tree, accordingly their importance with respect to the predictability of the target classes [63]. For the sake of readability they were scaled against the value of the most important layer, *variance 3x3* in our case. Even though a list of the different textures does not reveal much information about the generation of the RF model, the large proportion of textures of larger scales (25 and 69 pixels) indicates that they are of special use in our case. Generally they help to discriminate classes occurring at larger scales, especially when they are of similar texture such as open and closed shrubs. This was already found out by Woodcock and Strahler in 1987 [64].

Another essential point is the calculation of the texture layers. Antenna patterns may not be visible by the human eye but are necessarily to be removed before textures calculation. Otherwise they will be enhanced by the operator and cause extreme interference within the texture layers. These again will falsely train the RF classifier subsequently. This applies for both ERS and S1 data, but Single Look Complex (SLC) products of Sentinel-1 will instantly be corrected for azimuth bi-static delay, elevation antenna pattern and range spreading loss [65]. Lastly, also the integration of elevation data can enhance the accuracy, such as shown by Braun and Hochschild [42].

As the RF model of the year 2000 is applied to all other ERS scenes it is extremely sensitive to the values created. Accordingly, textures of all scenes must be calculated based on the same range of input values. In our case, we excluded the upper and lower 2.5% of the histogram of the scene from 2000 and used them as constant minimum and maximum values throughout all ERS input rasters. This assures that the value ranges of different textures remain the same for all input scenes and therefore stay transferable within the classifier [53].

The RF algorithm itself turned out to be helpful for the selection of both suitable textures and the integration of different kernels in order to model the distribution of the target classes. A crucial prerequisite is a sufficient number of training samples. These should not necessarily include all input classes to the same proportion but rather take their spatial occurrence into consideration. Thereby, a minimum sample size of 50 points per class is advisable and, as a matter of course, the larger the training data the higher is the power to detect finer differences [66].

Minor misclassifications are acceptable because they only slightly affect the later calculation of the NRD values of the corresponding cell. Each cell contains 10.000 classified pixels, so smaller errors caused by the nature of the SAR images mostly vanish within the resolution of the analysis grid. Additionally, as Table 3 demonstrates, most of the misclassifications occur between ecologically related classes which already have similar relative importance (RIs, see Table 2).

The achieved overall accuracy of 71 % is acceptable but could be increased in further studies. One option lies within the IW mode of Sentinel-1 data which operates at VV and VH polarizations.

These deliver further information about the form and structure of surface elements and of course can both be integrated in the RF algorithm. Another option is the use of the interferometric coherence gained by two scenes within a short period (12 days in best case for S1). It detects temporal variation between the two acquisitions and could therefore additionally support the discrimination of static from dynamic land-use / land cover classes such as forest types or flooded for instance [67,68].

Table 4. Feature importance of the input raster layers

Raster name	Size	Importance
Variance	3	100,0%
Difference Of Entropies	69	73,7%
Sum Variance	25	66,7%
IC2	69	58,8%
Energy	25	55,1%
IC1	25	52,8%
Haralick Correlation	25	50,3%
High Grey-Level Run Emphasis	69	43,6%
Sum Entropy	3	38,3%
Inertia	69	36,1%
Cluster Prominence	25	33,4%
Mean	25	31,1%
Difference Of Variances	3	30,1%
Mean	3	30,1%
Correlation	69	27,5%

Table 5. Areas of severe degradation around the refugee camps

	Beaodou et al. 2009 (1997)	This study (1997)
Dagahaley	21,8 km²	27,2 km²
Ifo	28,9 km²	28,9 km²
Hagadera	19,3 km²	17,8 km²
Dadaab	3,8 km²	4,2 km²

Regarding the NRD maps we expected a clearer image of land degradation. Apparently, that refugee camps are progressively 'carving' into their environment is not the case in Eastern Kenya. There are obvious consequences such as the expansion of bare soil areas and a slight but gradual decrease of shrubland which could be observed from the maps. But except for certain hot spots around the camps and in hydrologically affected areas a clear image of loss in the whole study area remains unconfirmed. Certainly, a study area with more distinct classes, such as investigated by Hagenlocher et al. [39], would also produce NRD maps of higher contrast when changes do occur between more distinctive classes of similar ecological importance. In fact our study area offered less potential for drastic developments between the chosen types of land-use and land cover. Studies located outside savannas with more complex ecosystems and noticeable borders between ground cover and forests for example should therefore lead to more pronounced NRD maps.

Altogether the approach produces plausible results. Many points indicate that the classification and generation of the Natural Resource Depletion Index are correct. For example, Enghoff et al. [69] report that flooding due to clayey soils mostly occurs around the camps Ifo and Dagahaley. Referring to Fig. 5 these are the areas with the highest positive and negative NRD values. They evidently occur due to temporarily flooding which causes an alternating of the classes *bare soil* and *floodplain* expressing in large fluctuations of the NRD. And maybe flooding is also the reason for the large overall increase of NRD for the period from 2005 to 2010 portrayed in section 3.3: UN Habitat reports of large floods which affected nearly 100.000 people of camp Ifo in the year 2006 [70]. These may have also had a larger effect on the surrounding floodplains and caused a wider ecologic profit in the study area which could cause the total NRD of 2010 to be not only above zero but also clearly positive (+8.13). However, although the number of people began to decrease since 2011 when a maximum of 454.000 people was reached land degradation continued until today as seen in Fig. 5d [71]. This corresponds to the prediction of Enghoff et al. [69] who claimed that although a reduction in the camp population would permit natural regeneration, large-scale rehabilitation of the hosting area would neither be technically nor financially feasible. According to that, a significant ecological benefit cannot be expected, despite of the fact that Kenya, Somalia and the UNHCR signed a treaty in 2013 that coordinates the return of Somali into their home country [72].

Looking at similar studies, Johannessen et al. [73], Füreder et al. [74] and Baker et al. [75] also used remote sensing images for the observation of areas with refugee camps, amongst others in Dadaab as well, but restricted their analyses to interpretations or classifications of camp structures based on very high resolution images, so the findings regarding environmental

conditions cannot be taken for comparison. Tachiiri and Ohta [76] investigated the environmental changes around Kakuma refugee camp in Northern Kenya where the landscape is comparably monotonous. They report a clear reduction of the *Normalized Differenced Vegetation Index* (NDVI) calculated from the NOAA/AVHRR satellite between 1989 and 1999. But they face distortions due to differences in precipitation as well. Beaudou et al. [77] assessed the area of degradation around the refugee camps for 1998. Their findings are presented in Table 3. A high general agreement with our results can be determined. Except for camp Dagahaley, where the area is overestimated by almost 25%, the outcomes of both studies are mutually confirmative.

4. CONCLUSIONS

This study presented an approach to assess changes in land-use / land cover and to estimate their ecologic impact. The used ERS data are free of atmospheric distortions and could therefore be compared due to thorough radiometrical and geometrical calibration. An additional scene from Sentinel-1 was used in order to include information of present conditions.

The proposed method proved suitable for multi-temporal analyses of changes within landscapes. Especially when there is a gain or loss in quality, the analysis grid can help to identify centers of transition between classes of different ecological importance. Still, the results are strongly dependent from the defined classes as well as the weights addressed to them. Of course, these weights could also address different domains such as agricultural suitability or livelihood security, for example. In our case land-use classes may have been to similar so the resulting maps of Natural Resource Depletion (NRD) did not directly explain a relation between the increasing number of refugees and the loss of ecological resources.

Nonetheless, a general decrease of resources has been detected for the time between 1997 and 2014, especially for certain hot spots. Additionally, an increasing of bare rocks and soil areas around the camps was observed. Their development not only reflects the growing of the camp areas but also corresponds to findings of other studies. Furthermore, the availability of fluvial water is essential in the study area as it controls the vegetation within the braided river system and the floodplain.

The Random Forest classifier was trained for the scene from 2000 and applied to the others whereat large scale textures played a major role for the discrimination of classes. Misclassifications mostly occurred between ecologically related classes.

The presented approach was developed for ERS data but also targets its later use with Sentinel-1. Since the middle of 2014 its number of freely available scenes in the *Scientific Data Hub* (https://scihub.esa.int) is gradually increasing. It can therefore be applied on S1 data for studies change detection or multi-temporal classifications of smaller time spans. However, this requires removal of antenna patterns and a reasoned selection of the used scenes: For studies covering several areas all images should be acquired within the same season, especially in arid areas with sparse precipitation. If the approach is used for a multi-temporal classification of single point in time importance should be placed on constant time intervals between the images and the incorporation scenes from both the dry and rainy seasons for best contrasts in SAR backscatter intensity.

Under these conditions, the presented approach is suitable for an operational use of SAR data for the long-term monitoring landscape resources around refugee camps.

ACKNOWLEDGEMENTS

This study was funded by the Austrian Research Promotion Agency (FFG) under the Austrian Space Applications Programme (ASAP 9, Nr. 840081). ERS data was provided by the European Space Agency. Sentinel-1 data was provided by Copernicus and the European Space Agency respectively. Landsat data was available from the U.S. Geological Survey.

COMPETING INTERESTS

Authors have declared that no competing interests exist.

REFERENCES

1. UNHCR. World at war. Global Trends 2014. United Nations High Commissioner for Refugees, Field Information and Coordination Support Section, Division of Programme Support and Management, Switzerland; 2015.

2. Lang S, Füreder P, Kranz O, Card B, Roberts S, Papp A. Humanitarian emergencies: Causes, traits and impacts as observed by remote sensing. In: Thenkabail P, editor. Remote Sensing Handbook, New York: Taylor and Francis. 2015;483–512.
3. Kenyon Lischer S. Dangerous Sanctuaries: Refugee Camps, Civil War, and the Dilemmas of Humanitarian Aid. 1st ed. New York: Cornell University Press; 2006.
4. Castles S, Miller M, Ammendola G. The age of migration: International population movements in the modern world. 4th ed. New York: Palgrave Macmillan; 2009.
5. Perouse de Montclos M, Kagwanja P. Refugee Camps or Cities? The socio-economic dynamics of the Dadaab and Kakuma Camps in Northern Kenya. J Refug Stud. 2009;13(2):205–222.
   DOI: 10.1093/jrs/13.2.205
6. Crea T, Calvo R, Loughry M. Refugee health and wellbeing: Differences between urban and camp–based environments in Sub-Saharan Africa. J Refug Stud. 2015; 28(3):319–330.
   DOI: 10.1093/jrs/fev003
7. Goodkind J, Foster-Fishman P. Integrating diversity and fostering interdependence: Ecological lessons learned about refugee participation in multiethnic communities. J Community Psychol. 2002;30(4):389–409.
   DOI: 10.1002/jcop.10012
8. Jacobsen K. Refugees' environmental impact: The effect of patterns of settlement. J Refug Stud. 2007;10(1):19–36.
   DOI: 10.1093/jrs/10.1.19
9. Nail T. The figure of the migrant. 1st ed. Stanford: Stanford University Press; 2015.
10. Juma K, Suhrke A. Eroding local capacity: International Humanitarian Action in Africa. 1st ed. Uppsala: Nordiska Afrikainstitutet; 2002.
11. Jacobsen K. Livelihoods in conflict. The Pursuit of Livelihoods by Refugees and the Impact on the Human Security of Host Communities. Int Migr. 2000;40(5):95–123.
   DOI: 10.1111/1468-2435.00213
12. Agier M. Between war and city. Towards an urban anthropology of refugee camps. Ethnography. 2002;3(3):317–341.
   DOI: 10.1177/146613802401092779
13. Crisp J. A state of insecurity: The political economy of violence in Kenya's refugee camps. Afr Aff. 2000;99:601–632.
   DOI: 10.1093/afraf/99.397.601
14. Kibreab G. Environmental causes and impact of refugee movements: A critique of the current debate. Disasters. 1997;21(1): 20–38.
   DOI: 10.1111/1467-7717.00042
15. Whitaker R. Refugees in Western Tanzania: The distribution of burdens and benefits among local hosts. J Refug Stud. 2002;15(4):339–358.
   DOI: 10.1093/jrs/15.4.339
16. Kranz O, Sachs A, Lang S. Assessment of environmental changes induced by internally displaced person (IDP) camps in the Darfur region, Sudan, based on multi-temporal MODIS data. Int J Remote Sens. 2015;36(1):190–210.
   DOI: 10.1080/01431161.2014.999386
17. Lang S, Tiede D, Hölbling D, Füreder P, Zeil P. EO-based ex-post assessment of IDP camp evolution and population dynamics in Zam Zam, Darfur. Int J Remote Sens. 2010;31(21):5709–5731.
18. Wulder MA, White JC, Goward SN, Masek JG, Irons JR, Herold M, Cohen WB, Loveland, TR, Woodcock CE. Landsat continuity: Issues and opportunities for land cover monitoring. Remote Sens Environ. 2008;112(3):955–969.
   DOI: 10.1016/j.rse.2007.07.004
19. Belward AS, Skøien JO. Who launched what, when and why; trends in global land-cover observation capacity from civilian earth observation satellites. ISPRS J Photogramm Remote Sens. 2015;103: 115–128.
   DOI: 10.1016/j.isprsjprs.2014.03.009
20. Knorn J, Rabe A, Radeloff, VC, Kuemmerle T, Kozak J , Hostert P. Land cover mapping of large areas using chain classification of neighboring Landsat satellite images. Remote Sens Environ. 2009;113(5):957–964.
   DOI: 10.1016/j.rse.2009.01.010
21. Vogelmann JE, Howard SM, Yang L, Larson CR, Wylie BK, Van Driel JN. Completion of the 1990's National land cover data set for the conterminous United States. Photogramm Eng Remote Sensing. 2001;67:650–662.
22. Fuller RM, Groom, GB, Jones AR. The land cover map of Great Britain: An

automated classification of Landsat Thematic Mapper data. Photogramm Eng Remote Sensing. 1994;60(5):553–562.

23. Haack B, Bryant N, Adams S. An assessment of landsat MSS and TM data for urban and near-urban land-cover digital classification. Remote Sens Environ. 1987; 21(2):201–213.
DOI: 10.1016/0034-4257(87)90053-8
24. Byrne GF, Crapper PF, Mayo KK. Monitoring land-cover change by principal component analysis of multitemporal landsat data. Remote Sens Environ. 1980;10(3):175–184.
DOI: 10.1016/0034-4257(80)90021-8
25. Zhu Z, Woodcock CE, Holdena C, Yang Z. Generating synthetic Landsat images based on all available Landsat data: Predicting Landsat surface reflectance at any given time. Remote Sens Environ. 2015;162:67–83.
DOI: 10.1016/j.rse.2015.02.009
26. De Fries RS, Hansen M, Townshend JRG, Sohlberg R. Global land cover classifications at 8 km spatial resolution: The use of training data derived from Landsat imagery in decision tree classifiers. Int J Remote Sens. 1998; 19(16):3141–3168.
DOI: 10.1080/014311698214235.
27. Ju J, Roy DP. The availability of cloud-free Landsat ETM+ data over the conterminous United States and globally. Remote Sens Environ. 2008;112:1196–1211.
DOI: 10.1016/j.rse.2007.08.011
28. Goward S, Arvidson T, Williams D, Faundeen J, Irons J, Franks S. Historical record of Landsat global coverage. Mission operations, NSLRSDA, and International Cooperator stations. Photogramm Eng Remote Sensing. 2006; 72(10):1155–1169.
DOI: 10.14358/PERS.72.10.1155
29. Warren SG, Hahn CJ, London J, Chervin RM, Jenne RL. Global distribution of total cloud cover and cloud type amounts over land. NCAR Technical Note NCAR/TN-273+STR; 1986.
Available:http://nldr.library.ucar.edu/repository/collections/TECH-NOTE-000-000-000-628
DOI: 10.5065/D6GH9FXB
30. Lin CH, Lai KH, Chen ZB, Chen JY. Patch-based Information Reconstruction of cloud contaminated multitemporal images. IEEE Trans Geosci Remote Sens. 2014;52(1): 163–174.
DOI: 10.1109/TGRS.2012.2237408
31. Richards JA. Remote Sensing with Imaging Radar. 1st ed. New York: Springer; 2009.
32. Waske B, Braun M. Classifier ensembles for land cover mapping using multitemporal SAR imagery. ISPRS J Photogramm Remote Sens. 2009;64(5): 450–457.
DOI: 10.1016/j.isprsjprs.2009.01.003
33. Haack B, Bechdol M. Integrating multisensor data and RADAR texture measures for land cover mapping. Comput Geosci. 2000;26(4):411–421.
DOI: 10.1016/S0098-3004(99)00121-1
34. Dobson MC, Ulaby FT, Pierce LE. Land-cover classification and estimation of terrain attributes using synthetic aperture radar. Remote Sens Environ. 1995;51(1): 199–214.
DOI: 10.1016/0034-4257(94)00075-X
35. Waring RH, Way J, Hunt ER, Morrissey L, Ranson KJ, Weishampel JF, Oren R, Franklin SE. Imaging radar for ecosystem studies. BioScience. 1995;45(10):715–723.
DOI: 10.2307/1312677
36. Martin A. Environmental conflict between refugee and host communities. J Peace Res. 2005;42(3):329–346.
DOI: 10.1177/0022343305052015
37. Lonergan S. The role of environmental degradation in population displacement. Environ Change Secur Proj Rep. 1998;4: 5–15.
38. Black R. Forced Migration and environmental change: The impact of refugees on host environments. J Environ Manage. 1994;42(3):261–277.
DOI: 10.1006/jema.1994.1072
39. Hagenlocher M, Lang S, Tiede D. Integrated assessment of the environmental impact of an IDP camp in Sudan based on very high resolution multi-temporal satellite imagery. Remote Sens Environ. 2012;126:27–38.
DOI: 10.1016/j.rse.2012.08.010
40. Ndyeshumba P. The use of Remote Sensing for environmental impact assessment and determination of the area affected by refugees in Ngara district North Western Tanzania. Int Arch J Photogramm Remote Sens. 2000;33(B7):981–984.
41. Lodhi MA, Echavarria FR, Keithley C. Using remote sensing data to monitor land

cover changes near Afghan refugee camps in northern Pakistan. Geocarto Int. 1998;13(1);33–39.
DOI: 1080/10106049809354626

42. Braun A, Hochschild V. Combining SAR and optical data for environmental assessments around refugee camps. In: Jekel T, Car A, Strobl J, Griesebner G, editors. Geospatial minds for society. Berlin: Wichmann; 2015;424–433.
DOI: 10.1553/giscience2015s424
43. Astrium GEO-Information Servies. Observation of Dadaab (Kenya) Refugee Camps with TerraSAR-X Radar Data. Unpublished presentation; 2011.
Available:http://www2.geo-airbusds.com/files/pmedia/public/r2337_9_201108_astriumgeo_terrasarx_dadaab_refugee_camp.pdf (Accessed 12 September 2015)
44. UNHCR. Dadaab refugee camps, Kenya. UNHCR bi-weekly updates, 16–31 August 2015.
Available:http://data.unhcr.org/horn-of-africa/download.php?id=1715 (Accessed 13 September 2015)
45. Salmio T. Refugees and the Environment: An Analysis and Evaluation of the UNHCR's Policies in 1992–2002. Faculty of Social Sciences, University of Turku, Finland; 2009.
Available:http://www.safefuelandenergy.org/files/Analysis%20of%20UNHCR's%20environment%20policies.pdf (Accessed 13 September 2015)
46. White F. The Vegetation of Africa. A descriptive memoir to accompany the Unesco/AETFAT/UNSO vegetation map of Africa. Natural Resources Research Report XX, UN Educational, Scientific and Cultural Organization, France; 1983.
47. ESA. ERS missions: 20 years of observing earth. ESA Communications, Netherlands; 2013.
Available:http://www.cmima.csic.es/files/webcmima/docs/biblio-pdf/doc_4190.pdf (Accessed 13 September 2015)
48. Torres R, Snoeij P, Geudtner D, Bibby D, Davidson M, Attema E, Potin P, Rommen B, Floury N, Brown M, Traver IN, Deghaye P, Duesmann B, Rosich B, Miranda N, Bruno C, L'Abbate M, Croci R, Pietropaolo A, Huchler M, Rostan F. The Sentinel Missions - New Opportunities for Science. Remote Sens Environ. 2012;120:9–24.
DOI: 10.1016/j.rse.2011.05.028
49. Small D. Flattening gamma: Radiometric terrain correction for SAR imagery. IEEE Trans Geosci Remote Sens. 2011;48(8): 3081–3093.
DOI: 10.1109/TGRS.2011.2120616
50. Loew A, Mauser W. Generation of geometrically and radiometrically terrain corrected SAR image products. Remote Sens Environ. 2007;106(3):337–349.
DOI: 10.1016/j.rse.2006.09.002
51. Collins MJ, Wiebe J, Clausi DA. The effect of speckle filtering on scale-dependent texture estimation of a forested scene. IEEE Trans Geosci Remote Sens. 2000; 38(3):1160–1170.
DOI: 10.1109/36.843008
52. Thenkabail PS, Gupta, RK. Texture based classification of multidate SAR images - A case study. Geocarto Int. 1998;13(3):53–62.
DOI: 10.1080/10106049809354652
53. Haralick RM, Shanmugam K, Dinstein I. Textural features for image classification. IEEE Trans Syst Man Cybern. 1973;3(6): 610–621.
DOI: 10.1109/TSMC.1973.4309314
54. di Gregorio A. Land cover classification system. Classification concepts and user manual. Food and Agriculture Organization of the United Nations, Rome; 2009.
Available:http://www.glcn.org/downs/pub/docs/manuals/lccs/LCCS2-manual_en.pdf (Accessed 15 September 2015)
55. Sandholt I, Möller Sörensen J, Rasmussen K, Ka A. The use of ERS2 SAR for assessment of changes in dry herbaceous biomass. Geoscience and Remote Sensing Symposium, IGARSS '02. 2002;4: 2002–2005.
DOI: 10.1109/IGARSS.2002.1026427
56. Blyth K. Seasonal changes in surface soil moisture and vegetation observed by ERS-1 SAR over temperate grassland and semi-arid savannah. IE Proceedings Vol. 2314: Multispectral and Microwave Sensing of Forestry, Hydrology, and Natural Resources 449; 1995.
DOI: 10.1117/12.200771
57. Zhang YJ. Machine learning for image classification. Encyclopedia of Information Science and Technology 3rd ed. Hershey, PA: IGI Global; 2015.
58. Breiman L. Random forests. Mach Learn. 2001;45(1):5–32.
DOI: 10.1023/A:1010933404324

59. Breiman L, Friedman JH, Olshen RA, Stone CJ. Classification and regression treees. 1st ed. Boca Raton, PA: CRC Press; 1984.
60. Amnesty International. 'No Place for us here'. Violence against refugee women in eastern Chad. London, UK: Amnesty International Publications; 2009. Available:http://www.amnesty.ie/sites/default/files/report/2010/04/Chad%20report.pdf (Accessed 09 September 2015)
61. Bloesch U. The use of fire in the environmental rehabilitation on the sites of a former refugee camp at Benaco, Tanzania. Schweiz Z Forstwes. 2001; 152(9):377–382. DOI: 10.3188/szf.2001.0377
62. Murni A, Darwis N, Mastur M, Hardianto D. A texture classification experiment for SAR radar images. Intern J Pattern Recognit Artif Intell. 1994;16:213–224. DOI: 10.1016/B978-0-444-81892-8.50023-7
63. Archer KJ, Kimes RV. Empirical characterization of random forest variable importance measures. Comput Stat Data Anal. 2008;52(4):2249–2260. DOI: 10.1016/j.csda.2007.08.015
64. Woodcock CE, Strahler AH. The factor of scale in remote sensing. Remote Sens Environ. 1987;21(3):311–332. DOI: 10.1016/0034-4257(87)90015-0
65. ESA. Sentinel-1. ESA's Radar Observatory Mission for GME Operational Services. ESA Communications, Netherlands; 2012. Available:https://sentinel.esa.int/documents/247904/349449/S1_SP-1322_1.pdf (Accessed 12 September 2015)
66. Foody GM. Sample size determination for image classification accuracy assessment and comparison. Int J Remote Sens. 2008; 30(29):5273–5291. DOI: 10.1080/01431160903130937
67. Askne J, Hagberg JO. Potential of interferometric SAR for classification of land surfaces Geoscience and Remote Sensing Symposium, IGARSS '93. 1993;3: 985–987. DOI: 10.1109/IGARSS.1993.322164
68. Dellepiane S, Bo G, Monni S, Buck C. SAR images and interferometric coherence for flood monitoring. Geoscience and Remote Sensing Symposium, IGARSS '00. 2000;6;2608–2610. DOI: 10.1109/IGARSS.2000.859656
69. Enghoff M, Hansen B, Umar A, Gildestadt B, Owen M, Obara A. In search of protection and livelihoods. Socio-economic and environmental impacts of Dadaab refucee camp on host communities. Ministry Of Foreign Affairs, Denmark; 2010. Available:http://kenya.um.dk/en/~/media/Kenya/Documents/Final%20Report30092010.ashx (Accessed 09 September 2015)
70. UN Habitat. Shelter projects 2009. International Federation of Red Cross and Red Crescent Societies, Geneva, Switzerland; 2010. Available:http://www.disasterassessment.org/documents/204800-Sheltercatalogue2009-EN.pdf (Accessed 18 September 2015)
71. UNHCR. Statistical Yearbook. United Nations High Commissioner for Refugees, Field Information and Coordination Support Section, Division of Programme Support and Management, Switzerland; 2011. Available:http://www.unhcr.org/51628f589.html (Accessed 12 September 2015)
72. Abu Sa'Da C, Bianchi S. Perspectives of refugees in Dadaab on returning to Somalia. Forced Migration Review, Refugee Studies Centre, Oxford, UK; 2014. Available:http://www.fmreview.org/en/crisis/abusada-bianchi.pdf (Accessed 25 September 2015)
73. Johannessen OM, Dalen Ø, Bjørgo E, Rost T, Bouchardy JY, Babikr M, Andersen G, Paulson S, Haglund A, Ordonez C, Sandven S. Environmental monitoring of refugee camps using high-resolution satellite images (EnviRef) - Final Report. Nansen Environmental and Remote Sensing Center (NERSC), Norway; 2001.
74. Füreder P, Hölbing D, Tiede D, Lang S. Monitoring refugee camp evolution and population dynamics in Dagahaley, Kenya, based on VHSR satellite data. 9th International Conference African Association of Remote Sensing of the Environment (AARSE), El Jadida, Morocco; 2012.
75. Baker IL, Card BL, Raymond NA. Satellite interpretation Guide. Displaced population camps. Harvard Humanitarian Initiative (HHI), UK; 2013. Available:http://reliefweb.int/sites/reliefweb.int/files/resources/Satellite%20Imagery%2

0Interpretation%20Guide.pdf. (Accessed 26 September 2015)

76. Tachiiri K, Ohta I. Assessing impact of a large-sized refugee camp on the local vegetation condition with remote sensing: A case study of Kakuma, Kenya. Geoscience and Remote Sensing Symposium, IGARSS '04. 2004;3:1547–1550.
DOI: 10.1109/IGARSS.2004.1370608

77. Beaudou A, Cambrézy L, Souris M. Environment, cartography, demography and geographical information system in the refugee camps Dadaab, Kakuma, Kenya. Final report. Institute of Research for Development (IRD), France; 2009.
Available:http://www.cartographie.ird.fr/publi/Refugies/Final_report.pdf. (Accessed 26 September 2015)

Peer-review history:
The peer review history for this paper can be accessed here:
http://sciencedomain.org/review-history/12304